

## A Haptic Control Interface for a Motorized Exercise Machine

Craig R. Carignan and Jonathan Tang

**Abstract**—A haptic interface is generated for a powered arm curl machine for modulating resistance “on-the-fly” during strength training and rehabilitation. Force signals from a load cell are input to an impedance loop based on the desired resistance law, which then outputs position commands to a servomotor. The kinematics between the actuator drive and arm curl angle are derived, and the admittance control implementation used for realizing the resistance laws is described. Preliminary experimental results are presented for viscous and inertial control laws.

### I. INTRODUCTION

Resistance training has long been recognized as key to increasing muscular strength and endurance for both athletic performance and neuromuscular rehabilitation. The greatest increase in strength is attained through high resistances for short durations, while low resistances for long durations tend to produce high muscular endurance [1]. Until the 1970s, free weights (e.g. barbells and dumbbells) and Universal Gyms utilizing weight stacks driven by cable-pulleys were the primary means of resistance training. During the fitness craze in the 1980s, Nautilus, Cybex, and other companies introduced exercise machines into fitness centers for higher volume training. The cadre of resistance devices commercially available now includes pulley-weight machines, spring reaction devices (spring or pneumatic pistons), frictional devices (fans or brakes), and free weights.

Many of these machines offer some variability in resistance over the range of motion to account for the strength potential of the arm or leg in different configurations. This adjustability is usually attained through a series of cams and levers that make it harder to push (or pull) the “weight” in positions of greater biomechanical advantage. Although these devices may offer a level of adjustability, several researchers have experimentally demonstrated that the machine torque profiles do not match the human strength curve [4]. In addition, machines also have other issues:

- Inertial resistance is not optimal because weights can be “thrown” which causes uneven force over the range of motion.
- Maximum resistance should be applied at every position in order to increase strength throughout the range.
- Exercises should closely resemble the motion being trained or rehabilitated, to increase strength.

This work was supported by the U.S. Army Telemedicine and Advanced Technology Research Center (TATRC), Ford Detrick, Maryland

C. Carignan is a research associate professor and J. Tang is a robotics engineer with the Imaging Science and Information Systems Center, Georgetown University, Washington DC 20057 USA  
crc32@georgetown.edu, jt96@georgetown.edu

- Concentric and eccentric motion are both effective at increasing strength.
- External movement of a disabled limb is still useful in restoring its function.

An actively-controlled exercise machine can help resolve many of these issues. Different types of resistances could be generated and varied over the range of motion. Bidirectional forces could be applied to realize eccentric as well as concentric exercise. A powered machine could be used as an assistive device in the beginning stages of physical therapy and then gradually change over to a resistive training device as strength increases. In addition, strength training could be tailored to individual strength curves, which could slowly be restored to normal following injury or surgery [13].

In this work, a commercial curl machine was motorized in order to actively control the resistance during elbow flexion exercises (see Fig. 1). Active control allows new resistance laws to be implemented that have noninertial and eccentric characteristics and may be hard to generate physically. Resistance can also be automatically adjusted over the range of motion and tuned to individual strength characteristics. In addition, data from onboard sensors can be used to produce performance measures and track patient progress.



Fig. 1. Keiser Arm Curl 250 retrofitted with UltraMotion actuator.

This article begins with a brief review in Section II of previous work in actively-controlled exercise machines. The actuator and drive system used in this study are described

in Section III and a kinematic model is developed. The hardware and control system architecture are outlined in Section IV. Preliminary experimental results for inertial and damping resistances are given in Section V. Conclusions on the implementation of the approach along with some directions for future research are given in Section VI.

## II. PREVIOUS WORK

The idea of allowing a user to dynamically “tune” machine resistance is not new. Keiser, Inc. has developed a product line that uses pneumatic pistons instead of weights to provide resistance. The exerciser pushes buttons on the handle to either increase or decrease air pressure in the piston, causing a corresponding increase or decrease in resistance. However, the subject primarily uses this feature as an alternative to moving a pushpin on a weight stack and rarely changes resistance over the course of a repetition.

A motorized version of this concept is the leg extension machine developed at the University of Connecticut [7]. An electric motor that drives two sprockets is used by the machine to engage a cam that increases or decreases the angle of motion of a weighted lever arm. This innovation allows the user to adjust the resistance at any instant during a movement by operating a switch mounted on a grasp handle. Although adjustable, the resistance is still inertial, and the device relies on the human to control the amount of weight.

Automatic control of exercise machines has also been explored. A microprocessor-controlled leg press machine was developed at Georgia Tech in the 1980s [2]. The device used hydraulic pistons that were able to exert up to 300 N of force and drive the lift bar in both vertical and horizontal directions. Thus, the machine was capable of not only tuning the force, but also allowing paths in a plane rather than along a fixed arc or straight line.

Advanced concepts for “smart” exercise machines were under development at UC Berkeley in the mid 1990s and tested on a crank apparatus [10]. Investigators implemented a controller in the form of a nonlinear dynamic damper that would interact passively (stably) with the user. The controller made use of a force-velocity biomechanical model to try to extract maximum power during an exercise and thus elicit more efficient training. These concepts were later implemented into tunable brakes for a Nordic Track machine and a stair stepper exercise machine but did not advance to the commercial development stage [14].

## III. DRIVE SYSTEM MODELING

In this study, an arm curl machine was chosen for the prototype exercise device. In addition to being a common upper body exercise, elbow flexion also involves only three major muscle groups: biceps brachii, brachialis, and brachioradialis [9]. Isolation of muscle groups will facilitate clinical evaluation of the machine. To accelerate the development process, a commercial exercise machine was retrofitted with an active drive system rather than building a new device from scratch. This strategy allowed the development to focus on controls and software rather than the hardware.

The commercial version of the Keiser Arm Curl 250 machine using a pneumatic piston to push on a lever which then pulls on the arm curl bar using a rubber belt attached at the other end of the lever as shown in Figure 2. To achieve the high control bandwidths required for this application, the piston assembly was replaced with an UltraMotion actuator, which consisted of a lead screw with 0.125 in (0.3175 cm) pitch driven by an electric motor. The lead screw had a 20 cm stroke (greater than the original piston) and was capable of moving approximately 45 cm/sec unloaded, and 20 cm/sec with a 445 N load.



Fig. 2. View of arm curl machine showing the linear actuator connected to lever and belt drive.

Because of the complexity of the cam, lever, and drive belt assembly and absence of mechanical drawings, the mapping between the lead screw displacement and the elbow flexion angle was determined experimentally. The motor was commanded to move in increments of 5000 encoder counts, and then the angle of the curl bar was read off a protractor suspended from the bar as shown in Figure 3. The results are plotted in Figure 4.

Since the relationship is nonlinear, a third order polynomial curve was fit to the data ( $R=0.99997$ ) resulting in the following approximation between the elbow flexion angle  $\phi$  (rad) and the lead screw displacement  $x$  (m)

$$\phi(x) = \phi_0 + 0.3337 + 17.275x - 58.407x^2 + 506.07x^3 \quad (1)$$

where  $\phi_0$  is the constant offset between the curl bar angle and arm flexion angle. The Jacobian, defined as  $J \equiv \partial\phi/\partial x$ , relates the elbow flexion velocity to the lead screw velocity and can be found by differentiating (1) with respect to  $x$  resulting in

$$J(x) = 17.275 - 116.81x + 1518.2x^2 + 0.0010069x^3 \quad (2)$$

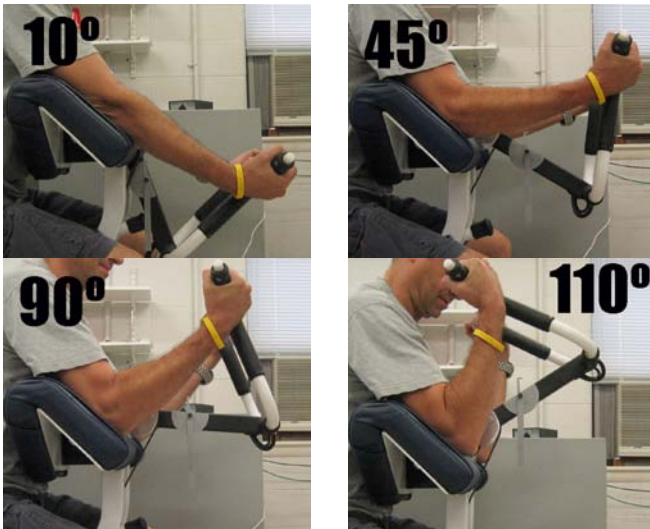


Fig. 3. Bicep curl repetition starting from near full extension through maximum flexion at about 110°. Protractor on arm curl bar was used to generate Figure 4.

The plot of the Jacobian versus the piston displacement is shown in Figure 5. As can be seen from the graph, the lead screw has minimum effect on the flexion angle at approximately 4 cm. By invoking the same duality found in manipulator kinematics [6], the Jacobian also relates the lead screw force  $F$  to the flexion torque  $\tau$

$$\dot{\phi} = J(x)\dot{x} \quad (3)$$

$$F = J(x)\tau \quad (4)$$

Thus (4) and (2) can be used to determine the torque produced by a given force at the lead screw. The graph in Fig. 6 shows the torque produced by a 500 N force at the piston versus the maximum isokinetic strength profile for elbow flexion [3] scaled to the same maximum peak value. (Note that since the original pneumatic piston on the Keiser machine produces constant force, the former is also the natural strength profile of the machine.) The plots illustrate the large discrepancy in elbow angle at which the maximum torque occurs. However, as stated in the introduction, maximum resistance should be applied at every position throughout the range of motion in order to increase strength, i.e., the human strength profile is optimum. The next section will describe the implementation of haptic interfaces for realizing common resistance laws at the elbow flexor joint.

#### IV. HAPTIC CONTROL INTERFACE

An UltraMotion lead screw actuator with an Animatics 1720 DC motor was used in place of the pneumatic piston in the original machine (see Fig. 7). The motor drives the lead screw via a rubber pulley with gear ratio 1:1 attached to the shaft. The angle of the motor is determined using a 2000 line incremental encoder mounted on the motor shaft. The encoder is read using the SmartMotor microprocessor which runs a servoloop at 2000 Hz based position commands sent over an RS232 line from the PC.

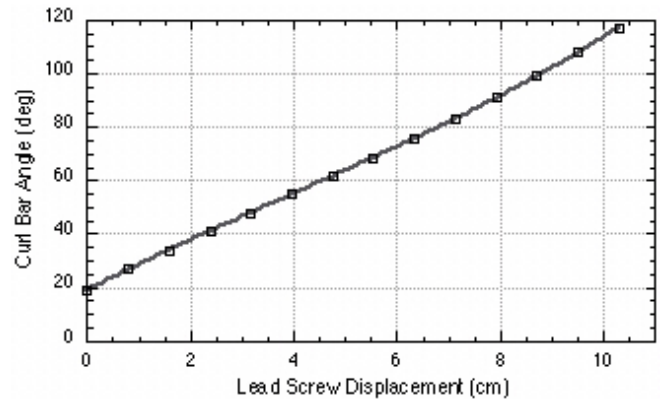


Fig. 4. Angle of curl bar versus the lead screw displacement.

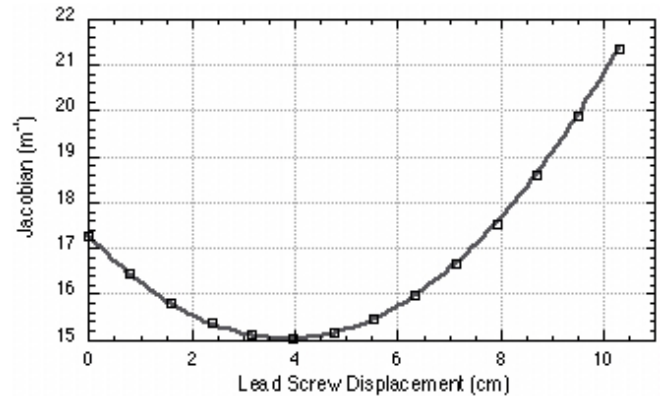


Fig. 5. Jacobian relating elbow flexion velocity to lead screw velocity.

A Sensotec Model 31 tension/compression load cell with 250 lb (1100 N) capacity was used to measure the force at the output of the actuator and was mounted between the output of the lead screw and the coupling to the lever arm on the machine (bottom left of Fig. 7). The load cell voltage and encoder were read directly by a National Instruments PCI-6013 16-bit data acquisition card in the PC rack and processed to produce position commands to be sent back to the SmartMotor by binary data transfer over the RS232 line.

The dual-loop admittance controller shown in Figure 8 was implemented using a PC and onboard microprocessor to control the drive assembly [12], [5]. This approach uses an outer loop wrapped around a force sensor to obtain the desired compliance, while a proportional-derivative (PD) servocontroller is used to drive the lead screw to the target position. Although model feedforward would help reduce the effect of friction and inertia in the drive system, the high PD gains in the servo controller reject most of these disturbances.

The impedance (outer) loop operates by using the force signal from the load cell  $F_s$  scaled by the desired admittance to produce a desired velocity  $\dot{x}_d$  command for the lead screw. The desired velocity is then integrated and multiplied by the gear ratio between the motor and lead screw drive  $\eta$  (0.3175 cm/rev) to obtain the desired angular position of the motor  $\theta_d$ . The commanded motor position is then sent from the PC over the serial line to the SmartMotor servocontroller to



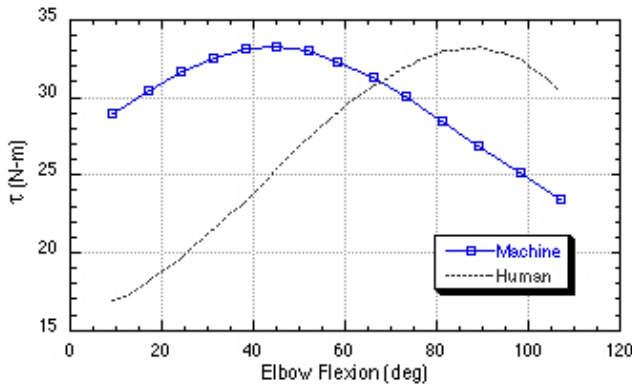


Fig. 6. Elbow flexion torque versus angle for constant force of 500 N applied at the lead screw. The human strength profile is shown for comparison. The force at the hand can be found by dividing the torque by the moment arm of 0.35 m.



Fig. 7. Keiser pneumatic piston (top) versus Ultramotion lead screw actuator driven by SmartMotor (bottom).

drive the lead screw to the desired position.

The resistance law is determined by the desired relationship between the applied force  $F$  and the velocity  $v$  at the handle. In general terms, this resistance is known as the mechanical “impedance”  $Z(s)$  [8] and is represented in the frequency domain as:

$$F(s) = Z(s)V(s) \quad (5)$$

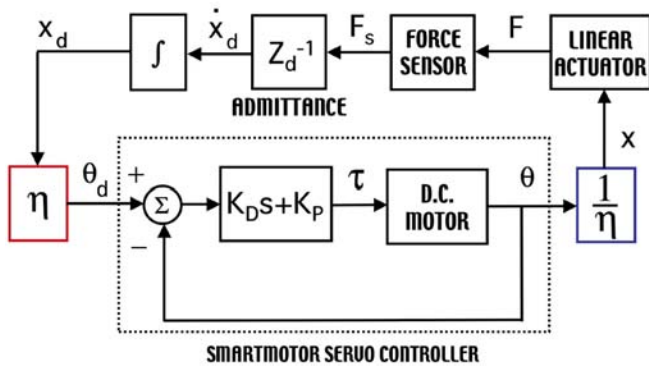


Fig. 8. Admittance control block diagram.

For the pure damper shown in Figure 9, the resistance law is given by

$$F(t) = b_d v(t) \quad (6)$$

$$Z(s) \equiv b_d \quad (7)$$

where  $b_d$  is the desired viscous damping coefficient. For the cable-pulley-weight system shown in Figure 10, the resistance law is given by

$$F(t) = m_d \dot{v}(t) - f_w \quad (8)$$

$$Z(s) \equiv m_d s \quad (9)$$

where  $m_d$  is the desired mass,  $g$  is the gravitational acceleration, and  $f_w = m_d g$ . (Note that the constant weight of the mass is not included in the impedance.) By contrast, the impedance for a pure spring would be the desired stiffness times the integral operator,  $Z(s) = k_d/s$ .

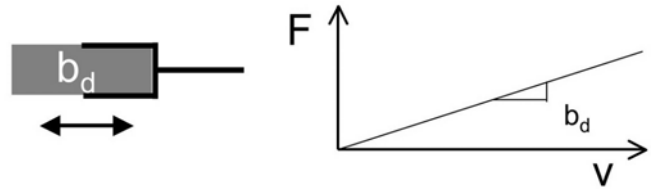


Fig. 9. Damping or “dashpot” resistance profile.

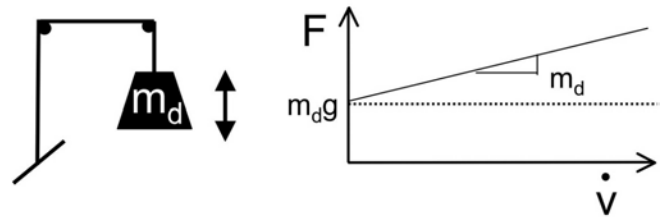


Fig. 10. Cable-weight resistance profile.

These fundamental impedance types can also be superposed to form more complex resistance laws such as the mass-spring-dashpot

$$Z(s) = m_d s + b_d + k_d/s \quad (10)$$

The next section presents some experimental results for inertial and damping impedances.

## V. ADMITTANCE CONTROL EXPERIMENTS

Two sets of preliminary experiments were conducted to validate operation of the exercise machine. In the first set, the admittance was set to be a pure resistive damper with an added bias force. In the second set, the admittance at the linear actuator was set to simulate a weight stack driven by a cable-pulley system. The sample rate of the PC was 150 Hz, and the SmartMotor sample rate was 2 KHz. A low pass filter with a bandwidth of 10 Hz was used to filter out force sensor noise and encoder noise due to backlash in the system.

### A. Viscous Damping

In these experiments, the desired impedance was a pure damper  $b_d = 2500$  N/m/s. A bias force of 200 N was also applied that exponentially rises to its final value with a decay constant of 0.5 cm. Thus, the desired force was

$$F_{des} = -2500\dot{x} - 200(1 - e^{-200(x-x_0)}) \quad (11)$$

The elbow flexion angle and lead screw velocity versus time are shown in Fig. 11. The flexion angle peaks at about  $100^\circ$ , and the velocity of the piston reaches a top speed of about 7 cm/s which is well within even its fully loaded capability.

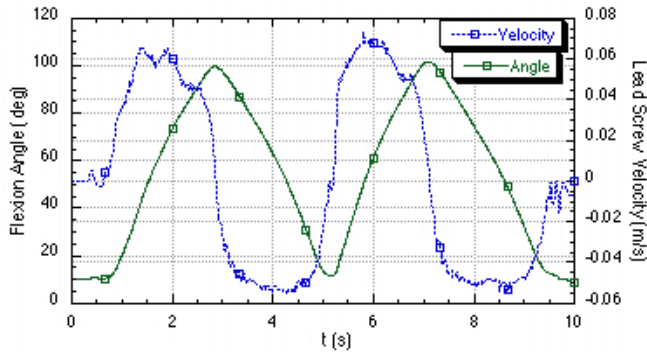


Fig. 11. Arm flexion angle and lead screw velocity during two repetitions with the damping controller.

The lead screw force versus time for two repetitions is shown in Fig. 12 alongside the velocity for reference. The bias force rises rapidly to 200 N, with the remainder of the applied force due to the damping impedance. The viscous damping peaks at about 150 N when the velocity reaches about 6 cm/s, which is consistent with a set damping of 2500 N/m/s. After the elbow begins extension (eccentric motion), the viscous force changes to the same direction as the bias force causing a large drop off in the force curve. As seen in the plot, the lead screw force tracks the desired force in (11) very closely throughout the motion.

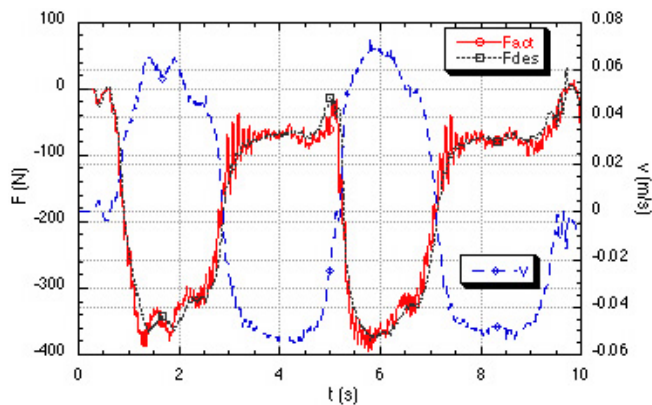


Fig. 12. Lead screw force and velocity versus time for the damping control law.

The resulting torque about the elbow versus the flexion angle for the two cycles is shown in Fig. 13. The top curve

is the concentric (flexion) phase, and the bottom curve is the eccentric (extension) phase. The concentric force peaks at approximately  $70^\circ$  which is midway between the human and machine peaks shown previously in Fig. 6.

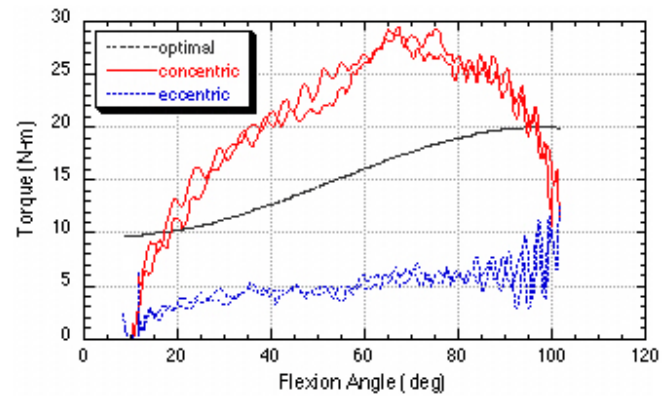


Fig. 13. Flexion torque versus angle for concentric and eccentric phases of the damping control experiment.

### B. Cable-Pulley-Weight Simulation

In these experiments, the machine was used to simulate an arm curl resistance provided by a mass on a cable-pulley system. Due to the sample rate limitations of the RS232 port, the controller was not stable for simulated masses below about 200 kg. Even a 6:1 reduction in force between the force applied at the lead screw and handle (moment arm = 0.355 m) would still result in too large of a weight to pull at the handle. Thus, the inertial mass,  $m_d$ , was set equal to 500 kg in (9), and the bias force  $f_w$  was set equal to 500 N, which is approximately equivalent to a 50 kg weight. Thus, the desired force was

$$F_{des} = -500\ddot{x} - 250 \quad (12)$$

The resulting elbow flexion angle and lead screw force versus time for a pair of arm curl repetitions is shown in Figure 14. The force averages about 250 N (the simulated weight), and the oscillations are characteristic of the undesirable acceleration and deceleration of the mass during elbow flexion and extension seen on many cable-pulley machines. From a subjective point of view, the controller provided a very realistic simulation of a cable-pulley machine although it was impossible to validate that forces were tracked correctly in the absence of acceleration measurements.

The resulting elbow torque as a function of the flexion angle is shown in Fig. 15. The concentric torques at the start of the motion are larger than in the eccentric phase due to the forces needed to accelerate the mass from rest but are correspondingly lower near the peak when the mass reverses direction. The eccentric torques are higher on average in the cruise phase because of the inertial deceleration forces. The torque peaks at approximately  $70^\circ$  which is significantly less than the isokinetic human strength profile superposed on the same graph.

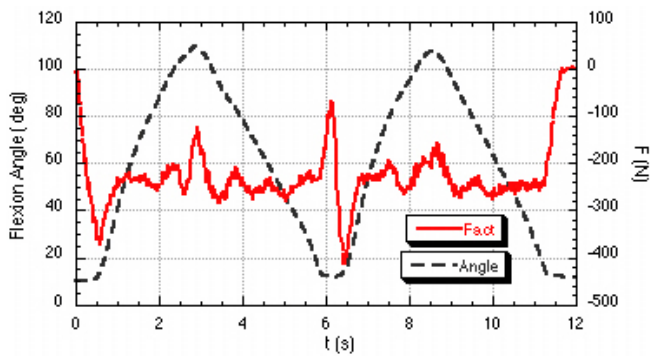


Fig. 14. Flexion angle and lead screw force versus time for cable machine test.

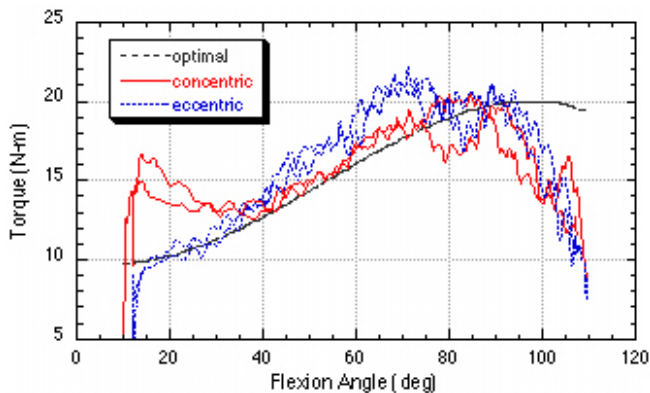


Fig. 15. Flexion torque versus angle for cable machine test.

## VI. CONCLUSIONS

A powered exercise machine was developed by retrofitting a commercial arm curl machine with a motorized lead screw drive. An optical encoder and load cell provided sensory feedback to a dual-loop admittance controller implemented on a PC and microprocessor. A 10 Hz low-pass filter was used to suppress electrical noise introduced into the system through the force sensor. Sample rates of the compliance loop were limited to 150 Hz by the RS232 communications link with the SmartMotor, which places an upper bound on the admittance gains that could be simulated. Fortunately, resistance training typically requires high impedance, which drives admittance toward the low end of the spectrum.

Experiments conducted with constant damping and force bias produced a smooth controlled motion, comparable to that of the original machine. The forces produced by the admittance controller accurately tracked the desired forces indicating that the desired damping was achieved. The peak torque occurs at a larger flexion angle than that of a constant force piston, but the peak still falls short of the isometric strength peak near  $90^\circ$ . This is because of the zero boundary condition of the damping resistance at maximum flexion and extension when the velocity goes to zero.

The machine was also used to simulate inertial resistance training using a cable-pulley-weight system. The experiment produced a very realistic haptic interface to the user, even faithfully replicating the “throwing” motion of the weight

stack on a cable often cited as a significant disadvantage of inertial training. Although our goal was to simply emulate an inertial trainer, the oscillations could be reduced or even eliminated by adding some damping to the desired impedance.

Our goal was to show that a motorized exercise machine could be used to achieve a wide variety of resistance laws, and this was demonstrated using damping and inertial resistance laws to simulated classes of well-known passive machines. The next step is to utilize this capability to develop resistance laws that closely match the human strength profile. As was shown here, it is not possible to match the human strength curve using linear impedances due to the hyperbolic-like relationship between muscle force and velocity first noted by Hill [11]. We are currently investigating the variable damping approach developed the team at UC Berkeley in the 1990s [10] for implementation on the arm curl machine, which may require reconfiguring the controller in an impedance implementation.

## ACKNOWLEDGMENT

Thanks go to Stephen Roderick and Jean-Marc for their software help and to Mike Perna who made new fittings for the machine. This project was sponsored by the U.S. Army Telemedicine and Advanced Technology Research Center (TATRC) under Grant #W81XWH-04-1-0078.

## REFERENCES

- [1] E. Aaberg, *Strength, Speed & Power*. Indianapolis: Alpha Books, 2002.
- [2] W. Book and D. Ruis, “Control of a robotic exercise machine,” in *Proceedings of the Joint Automatic Control Conference*, 1981, pp. WA-2A.
- [3] T. S. Buchanan, S. L. Delp, and J. A. Solbeck, “Muscular resistance to varus and valgus loads at the elbow,” *ASME Journal of Biomechanical Engineering*, vol. 120, pp. 634–639, Oct. 1998.
- [4] L. Cabell and C. J. Zebas, “Resistive torque validation of the nautilus multi-biceps machine,” *Journal of Strength and Conditioning Research*, vol. 13, no. 1, pp. 20–23, 1999.
- [5] C. Carignan and D. Akin, “Achieving impedance objectives in robot teleoperation,” in *Proc. of the IEEE Conference on Robotics and Automation*, 1997, pp. 3487–3492.
- [6] J. Craig, *Introduction to Robotics: Mechanics and Control*, 2nd ed. Reading, Mass.: Addison-Wesley, 1989.
- [7] F. Hatfield, “A new weights machine with dynamically adjustable resistance,” *Sportscience*, vol. 3, no. 1, 1999. [Online]. Available: <http://www.sportsci.org/jour/9901/fch.html>
- [8] N. Hogan, “Impedance control: An approach to manipulation,” *J. of Dynamics Systems, Measurement, and Control*, pp. 1–24, Mar. 1985.
- [9] E. Kneibbaum and K. M. Barthels, *Biomechanics: a qualitative approach for studying human movement*, 4th Ed. Boston: Allyn and Bacon, 1996.
- [10] P. Li and R. Horowitz, “Control of smart exercise machines,” *IEEE/ASME Transactions on Mechatronics*, vol. 2, no. 4, pp. 237–258, dec 1997.
- [11] R. Lieber, *Skeletal Muscle Structure and Function*. Baltimore: Williams and Wilkins, 1996.
- [12] J. Maples and J. Becker, “Experiments in force control of robotic manipulators,” in *Proc. of the IEEE Conference on Robotics and Automation*, Apr. 1986, pp. 695–702.
- [13] K. R. Saul, W. M. Murray, V. R. Hentz, and S. L. Delp, “Biomechanics of the steindler flexorplasty surgery: A computer simulation study,” *The Journal of Hand Surgery*, vol. 28A, no. 6, pp. 979–986, Nov. 2003.
- [14] J. Shields and R. Horowitz, “Adaptive step rate control of a stair stepper exercise machine,” in *Proceedings of the American Control Conference*, Philadelphia, jun 1998, pp. 1058–1062.